ACS OMEGA

Open Access

http://pubs.acs.org/journal/acsodf

Article

Nitrogen Recovery through Dissimilatory Nitrate Reduction to Ammonium: Impact of Environmental Factors

Teng-Fei Ma, Xiao-Yao Yu, Chong-Yang Xing, Zhen Liu, Zhen-Jun Wu,* and You-Peng Chen

Cite This: *ACS Omega* 2025, 10, 16695−16704

Read Online

ACCESS | Metrics & More | Article Recommendations | Supporting Information

ABSTRACT: The application of the bacterial dissimilatory nitrate reduction to ammonium (DNRA) process for treating nitrate-rich wastewater offers an environmentally friendly and resource-efficient strategy with significant potential for ammonium nitrogen recovery. This study investigates the impact of carbon sources, C/N ratios, pH, and temperature on the DNRA efficiency of *Pseudomonas* sp. strain LZ-1 (strain LZ-1). The results revealed that sodium citrate is the most favorable carbon source among sodium formate, sodium acetate, sodium propionate, and sodium citrate for enhancing DNRA in strain LZ-1. Ammonia production by strain LZ-1 peaks at a C/N of 8 within the range of 3 to 20, increasing before and decreasing thereafter. Furthermore, neutral to alkaline conditions (pH 7−10) are favorable for the DNRA process, with an optimal initial pH of 9. Temperature studies indicate a similar trend of initial increase followed by a decline in DNRA efficiency as temperatures rise from 20 to 35 °C, with peak ammonia production at 30 °C. The presence of sulfur ions inhibits the DNRA process in the strain LZ-1. However, this inhibitory effect diminished as the S/N ratio increased from 1/4 to 1. These insights contribute to a deeper understanding of the impact of environmental factors on DNRA and serve as a valuable reference for the utilization of strain LZ-1 in nitrogen recovery from nitrate-rich wastewaters.

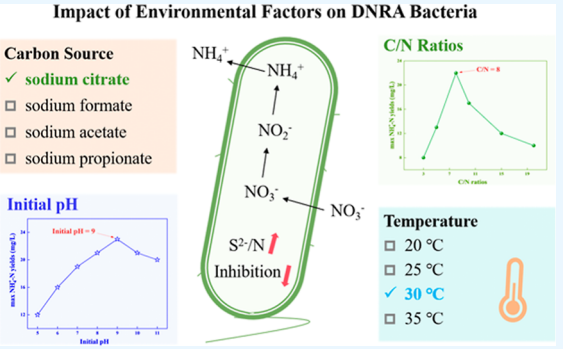

1. INTRODUCTION

For more than a hundred years, the Haber−Bosch process has been the cornerstone of ammonia (NH_3) production, accounting for roughly 95% of global output. This groundbreaking process has enabled the large-scale manufacture of fertilizers and a myriad of other nitrogen-based compounds that are essential to modern agriculture and industry.[1] Once synthesized through the Haber−Bosch method, ammonia can be readily neutralized, transforming into NH_4^+ when exposed to acidic conditions, a conversion that is vital for its subsequent use in various chemical processes.[2,3] Despite its pivotal role in the chemical industry, the Haber−Bosch process is not without its drawbacks. It is known for its high energy consumption, which contributes to a considerable carbon footprint, and the conversion efficiency of the process leaves room for improvement.[4] In light of these environmental and economic concerns, there has been a growing impetus to investigate and develop more sustainable, "green" alternatives for ammonia synthesis. Researchers are focusing on innovative methods that aim to reduce the energy requirements and carbon emissions associated with ammonia production, thereby paving the way for a more ecofriendly and efficient means of creating this crucial compound.

In this context, biological nitrogen conversion pathways have emerged as promising alternatives. Among these, dissimilatory nitrate reduction to ammonium (DNRA) represents a critical but often overlooked route in the nitrogen cycle.[5,6] Unlike denitrification, which converts nitrate (NO_3^-) to gaseous nitrogen (N_2) through intermediates like nitrous oxide (N_2O), DNRA reduces NO_3^- to bioavailable ammonium (NH_4^+) via two key enzymatic steps. The first phase reduces NO_3^- to nitrite (NO_2^-) via membrane-bound nitrate reductase (Nar) or periplasmic nitrate reductase (Nap).[7] The second phase involves NO_2^- reduction to NH_4^+, mediated by distinct pathways: (1) cytoplasmic NADH-dependent nitrite reductase (NirB) in the Nar/Nir pathway, (2) periplasmic cytochrome *c* nitrite reductase (NrfA) in the Nap/Nrf pathway, and (3) the reverse hydroxylamine:ubiquinone reductase module (rHURM) pathway, which employs hydroxylamine (NH_2OH) intermediates.[8−11] DNRA pathways vary based on electron donors and microbial species.[12,13] For instance, fermentative DNRA utilizes organic carbon (e.g., glucose, acetate) to generate NADH via glycolysis, providing electrons for NO_3^- reduction.[14,15] Conversely, chemolithoautotrophic DNRA employs inorganic donors like sulfide (S^{2-}) or Fe (II), where sulfide oxidation via enzymes like sulfide:quinone

Received: January 16, 2025
Revised: February 25, 2025
Accepted: April 11, 2025
Published: April 16, 2025

oxidoreductase (SQR) supplies electrons.[16,17] The novel pathway, rHURM, was recently discovered in *Nautilia profundicola*, which reduces NO_3^- to NH_4^+ via NH_2OH intermediates.[18] In wastewater treatment, DNRA can facilitate the total nitrogen removal by coupling with anammox, where NH_4^+ produced via DNRA serves as a substrate for anammox.[19,20] However, from this perspective, it appears that the significant potential of the DNRA process in effectively recovering ammonia from wastewater is not being fully utilized.

Wastewater containing high concentrations of nitrate can serve as a significant source for ammonia recovery.[21,22] However, during wastewater treatment, nitrate is often removed as a pollutant via denitrification, which converts it to N_2, leading to substantial losses of biologically available nitrogen.[23] In contrast to denitrification, the DNRA process can convert NO_3^--N to NH_4^+-N while preventing the emission of the greenhouse gas N_2O.[24] Subsequently, ammonium nitrogen in water can be recovered through physical and chemical methods, such as ion exchange and adsorption, or by adjusting the pH to convert ammonium nitrogen into ammonia gas, ultimately yielding ammonium salts for agricultural fertilizers. Thus, using the DNRA process to treat nitrate-rich wastewater for ammonium nitrogen recovery represents a green and resource-efficient approach with promising application potential.

In recent years, researchers have attempted to harness the DNRA process for ammonia recovery. For instance, Zhao et al. investigated the performance of a DNRA system within a membrane bioreactor, reporting a maximum ammonia nitrogen conversion efficiency of 92.05% when using ethanol as the carbon source with a COD/N ratio of 7.7.[25] Similarly, Wan et al. applied the DNRA process in a microbial fuel cell to treat nitrate nitrogen wastewater, achieving a maximum DNRA efficiency of 44%.[26] In the study conducted by Wang and colleagues, DNRA bacteria were successfully enriched in a nonwoven fabric membrane bioreactor under high C/N ratios, leading to an ammonia production efficiency from nitrate of 60.65%.[27] These studies highlight the feasibility of converting nitrate/nitrite to ammonium for subsequent recovery within bioreactor systems.

It is important to note that there exists a competitive relationship between denitrification and DNRA due to similar substrates and environmental conditions required for both processes.[14] Therefore, a detailed study of the factors influencing the DNRA process is crucial for enhancing its competitive advantage over denitrification and fully utilizing DNRA for ammonia nitrogen recovery. Previous research has indicated that various factors, including carbon source,[28,29] carbon-to-nitrogen ratio,[30] sulfide,[31] temperature,[32] pH,[33,34] and sludge age,[35] can influence the competition between DNRA and denitrification.[36] For example, Zhao et al. compared the performance of a DNRA system using sodium succinate, glucose, and ethanol as carbon sources, revealing that the highest ammonia nitrogen production efficiency occurred when ethanol was used with a COD/N ratio of 7.7.[25] Chutivisut et al. found that when glucose was the carbon source with a COD/NO_3^--N = 8:1, the microbial community in a sequencing batch reactor predominantly consisted of DNRA bacteria.[37] Previous studies found that a high S^{2-}/NO_3^- ratio typically promotes the DNRA process, while a low ratio favors the denitrification process.[38−40] This is because sulfur ions can serve as electron donors in the reduction of nitrate to ammonium, while simultaneously inhibiting the conversion of N_2O to nitrogen gas, the final step of denitrification.[39−41] Murphy et al. observed that increasing S^{2-} concentrations increased the activities of DNRA bacteria while diminished the denitrification process by lowering the abundance of denitrifiers in coastal environments.[42] The existence of SO_4^{2-} has also been reported to influence the DNRA process. Tuerk and Aelion reported that high concentrations of SO_4^{2-} in wetlands facilitated an increase in ammonia production rates via DNRA.[43] However, the inhibition of SO_4^{2-} to DNRA bacteria has also been observed.[44] Lai et al. demonstrated that within a temperature range of 10 to 40 °C, higher temperatures favored the DNRA process in soil.[45] Despite the growing interest in DNRA in recent years, knowledge of the environmental factors influencing the DNRA process, especially the DNRA bacteria, remains relatively limited.

To further enrich the understanding of the DNRA process and its influencing factors, this study utilized a DNRA bacterium, *Pseudomonas* sp. strain LZ-1 (strain LZ-1), isolated from activated sludge in a wastewater treatment plant (details of the isolation and identification process are provided in the Supporting Information), as an example. The aim was to investigate the effects of various environmental factors, including the carbon source, the carbon-to-nitrogen ratio, the initial pH, the temperature, and the S^{2-}/N ratio, on the DNRA process of strain LZ-1. The findings help to deepen the understanding of how environmental factors impact DNRA and provide some insights for the future application of strain LZ-1 in nitrogen recovery from nitrate-rich wastewater.

2. MATERIALS AND METHODS

2.1. Strain Screening and Culture. The DNRA bacterial strain LZ-1, employed in this research, was sourced from activated sludge within the secondary sedimentation tank at the Matougang Sewage Treatment Plant, located in Zhengzhou, Henan Province, China. The isolation and identification process are detailed in the Supporting Information. The gene sequence has been uploaded into the GenBank database with the accession number of OQ711934. The enrichment culture medium for the strain is beef extract peptone broth, which contains (per liter) 10 g of peptone, 5 g of sodium chloride, and 5 g of beef extract 5 g. The DNRA characteristics were investigated using SM medium or a modified SM medium. The SM medium contains (per liter) KNO_3 1.0 g, KH_2PO_4 1.0 g, $MgSO_4{\cdot}7H_2O$ 1.0 g, $FeC1_3{\cdot}6H_2O$ 0.05 g, and $CaC1_2{\cdot}2H_2O$ 0.2 g. Therefore, the concentration of nitrate nitrogen in the culture medium is 138.6 mg/L. The modified SM medium was developed based on the SM medium formulation by substituting 1.0 g of $MgSO_4{\cdot}7H_2O$ with 0.69 g of $MgCl_2{\cdot}6H_2O$, while all other components remained unchanged, thus yielding the modified SM medium. The reason for this substitution is to eliminate sulfur interference, since the modified SM medium is to be used in the S/N experiment (Section 2.4). The carbon source was added to the medium as required. The pH was adjusted to 7.0. Degassing of the oxygen in the medium was conducted by purging with nitrogen. All the media were autoclaved at 121 °C for 15 min. Culture medium storage, inoculation of bacteria, and sealing culture bottles with film and rubber stoppers are all conducted within an anaerobic chamber.

2.2. Carbon Source and Carbon-to-Nitrogen Ratio Experiments. To investigate the effect of different carbon

https://doi.org/10.1021/acsomega.5c00470
ACS Omega 2025, 10, 16695−16704

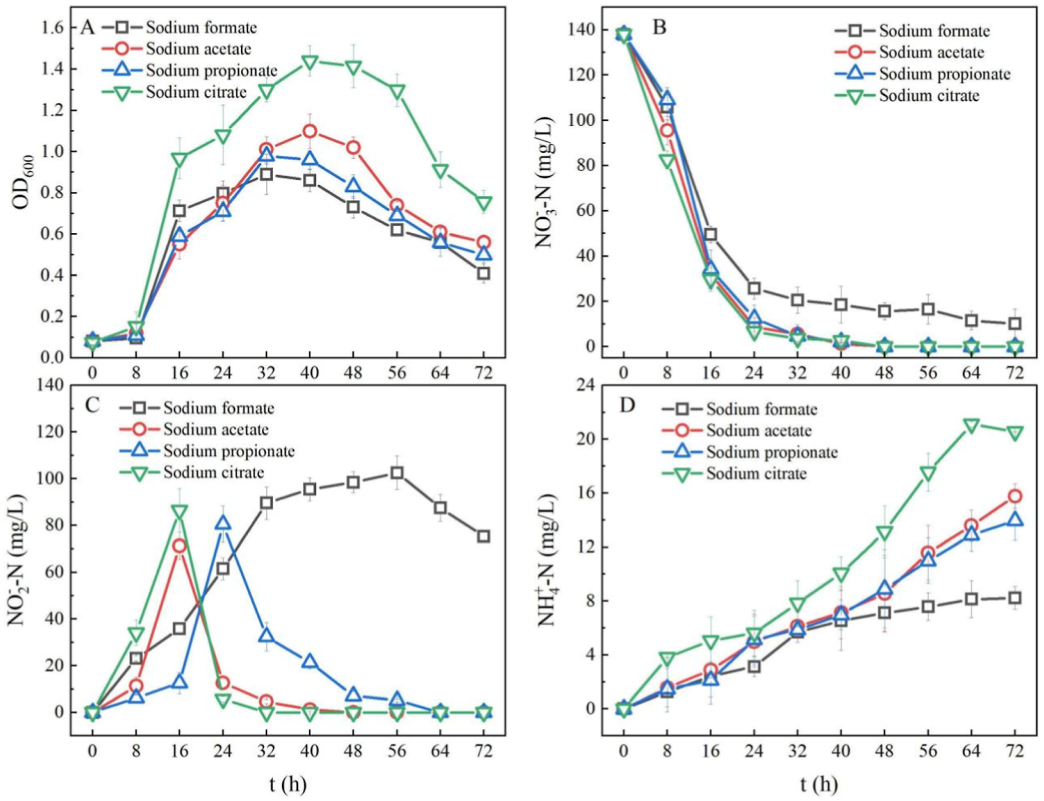

Figure 1. Cell growth and nitrate nitrogen transformation of strain LZ-1 under different carbon source conditions. (A) Changes in OD_{600}, (B) NO_3^--N concentrations, (C) NO_2^--N concentrations, and (D) ammonia nitrogen concentration.

sources on DNRA, sodium formate ($NaHCO_2$), sodium acetate ($NaC_2H_3O_2$), sodium propionate ($NaC_3H_5O_2$), and sodium citrate ($Na_3C_6H_5O_7$) were selected as additional carbon sources and added to the SM medium at a C/N ratio of 8, which means that the COD of the medium is 1108.8 mg/L. To evaluate the impact of C/N ratios on DNRA, the optimized carbon source determined from the different carbon source experiments was used for the varying C/N ratio experiments. The carbon source was adjusted into the SM medium to achieve C/N ratios of 3, 5, 8, 10, 15, and 20. For these experiments, strain LZ-1 was initially cultured in an enrichment medium until it reached an optical density at 600 nm (OD_{600}) of about 1. Subsequently, this culture was used to inoculate conical flasks filled with 100 mL of sterilized SM medium for anaerobic cultivation at 30 °C. All experimental procedures were carried out with three replicates.

2.3. Influence of Initial pH and Temperature on the DNRA Process of Strain LZ-1. In the initial pH influence experiment, the initial pH of the SM medium was set as 5, 6, 7, 8, 9, 10, and 11. The culture temperature was set at 30 °C. For the temperature influence experiment, the culture temperatures were set at 20, 25, 30, and 35 °C, with the optimal pH selected from the initial pH experiment. SM medium was prepared with the optimized carbon source and C/N ratio. The strain LZ-1 was initially cultured in the enrichment medium to an OD_{600} of approximately 1 and then inoculated into 100 mL of sterilized SM medium in conical flasks for anaerobic cultivation at 30 °C. All experiments were carried out in triplicate.

2.4. Influence of S^{2-}/N on the DNRA Process of Strain LZ-1. In the experiment investigating the impact of S^{2-}/N on the DNRA process of strain LZ-1, the modified SM medium was utilized. The optimized carbon source was added into the modified SM medium as the additional carbon source, maintaining a C/N ratio of 8. The S/N (S^{2-}) ratios were set at 1, 1/2, 1/3, and 1/4, which correspond to sulfur ion concentrations of 138.6 mg/L, 69.3 mg/L, 46.2 mg/L, and 34.7 mg/L, respectively. The pH level of the medium was meticulously adjusted to its optimal parameter utilizing 1 M HCl and 1 M NaOH. The strain LZ-1 was initially cultured in the enrichment medium to an OD_{600} of approximately 1 and then inoculated into 100 mL of sterilized medium in conical flasks for anaerobic cultivation at 30 °C. All experiments were conducted in triplicate.

2.5. Analytical Methods. The growth of strain LZ-1 is evaluated by measuring the OD_{600} of the bacterial culture broth. The concentrations of NH_4^+-N, NO_3^--N, NO_2^--N, S^{2-}, and SO_4^{2-} were determined following standard methods.[46] The NH_4^+-N yield efficiency is defined as the conversion efficiency of nitrate nitrogen to ammonia nitrogen. All experiments were performed in triplicate.

3. RESULTS AND DISCUSSION

3.1. Influence of Carbon Sources on the DNRA Performance of Strain LZ-1. The effects of different carbon sources ($NaHCO_2$, $NaC_2H_3O_2$, $NaC_3H_5O_2$, and $Na_3C_6H_5O_7$) on the cell growth and nitrate nitrogen transformation of strain LZ-1 were evaluated, as shown in Figure 1. As illustrated in Figure 1A, the growth of strain LZ-1 was optimal when sodium citrate was employed as the carbon source, with both growth rate and culture density throughout the cultivation period exceeding those observed with the other three carbon sources ($NaHCO_2$, $NaC_2H_3O_2$, and $NaC_3H_5O_2$). When sodium formate served as the carbon source, strain LZ-1 reached the stationary phase at 24 h, with a maximum culture density of

https://doi.org/10.1021/acsomega.5c00470
ACS Omega 2025, 10, 16695−16704

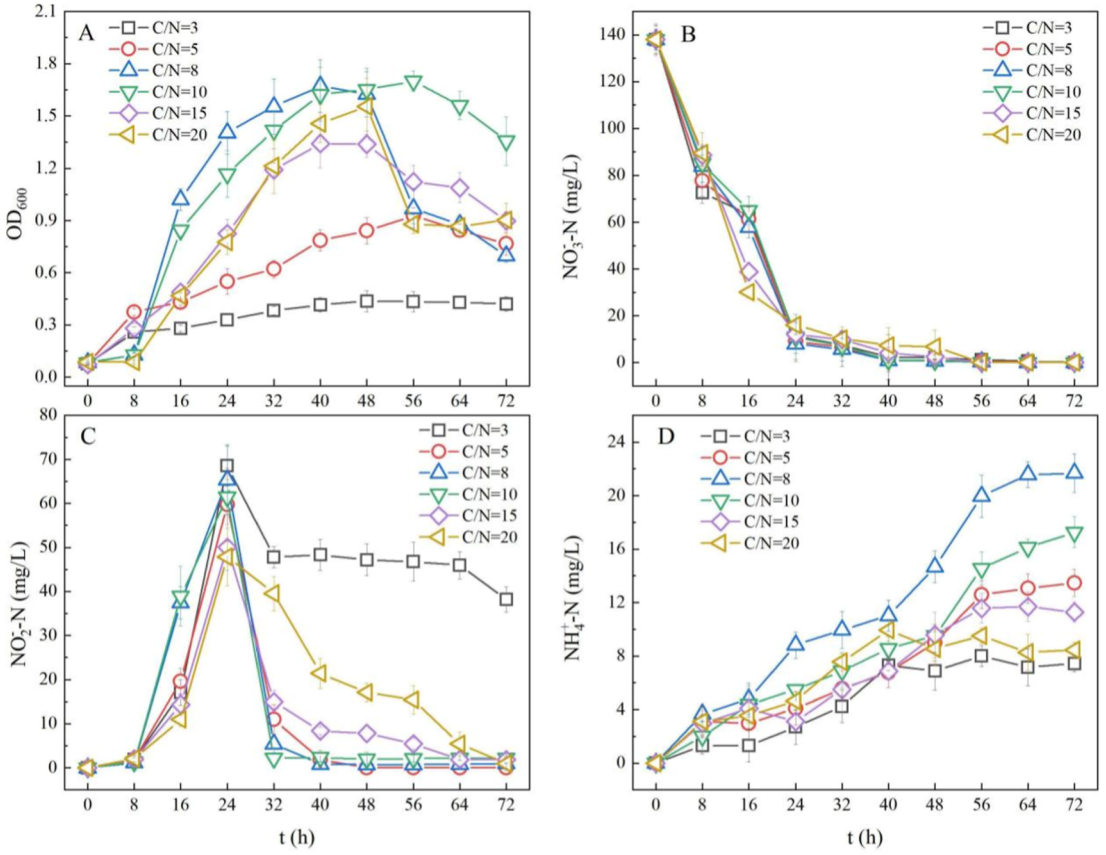

Figure 2. Cell growth and nitrate nitrogen transformation of strain LZ-1 under different C/N ratios. (A) Changes in OD_{600}, (B) NO_3^--N concentrations, (C) NO_2^--N concentrations, and (D) ammonia nitrogen concentration.

OD_{600} value of 0.89 at 32 h, which is the lowest recorded among all four carbon sources tested. Figure 1B shows that when sodium acetate, sodium propionate, and sodium citrate were used as carbon sources, strain LZ-1 exhibited effective removal of NO_3^--N, achieving a 100% removal efficiency after 48 h of cultivation. In contrast, the removal of NO_3^--N was less effective with sodium formate as carbon sources, with 7.30% of NO_3^--N remaining unremoved at 72 h. As seen in Figure 1C, when sodium citrate, sodium acetate, and sodium propionate were used as the carbon sources, the production of NO_2^--N by strain LZ-1 rapidly accumulated, reaching peak concentrations of 86.36 mg/L, 71.25 mg/L, and 80.56 mg/L at 16 h, respectively. Subsequently, the NO_2^--N concentration decreased rapidly to 0 mg/L at 32, 48, and 64 h. In contrast, when sodium formate was used, NO_2^--N continuously accumulated over 56 h, peaking at 102.56 mg/L before gradually declining to 75.23 mg/L by 72 h. Figure 1D indicates that the highest concentrations of NH_4^+-N produced by the strain LZ-1, using $NaHCO_2$, $NaC_2H_3O_2$, $NaC_3H_5O_2$, and $Na_3C_6H_5O_7$, were 8.23 mg/L, 15.77 mg/L, 13.96 mg/L, and 21.12 mg/L, respectively. The highest NH_4^+-N yield efficiency, 15.25%, was reached when sodium citrate was used as the carbon source.

These results demonstrate sodium citrate's superiority among tested carbon sources in enhancing DNRA efficiency of strain LZ-1, evidenced by optimized biomass growth, complete nitrate reduction, negligible nitrite accumulation, and maximal NH_4^+-N yield. This aligns with established carbon source-dependent regulation of dissimilatory nitrate reduction pathways.[36,47] The enhanced DNRA performance correlates with sodium citrate's biochemical characteristics: its tricarboxylic structure facilitates both direct transmembrane transport and TCA cycle integration, thereby supplying sustained NADH production required for the eight-electron nitrate-to-ammonium conversion.[48] Comparative studies by Carlson et al.[29] validate this substrate hierarchy, reporting terrestrial microbial consortia exhibited similar ammonium production patterns (citrate > acetate > propionate) under equivalent C/N ratios. The metabolic preference for citrate derivatives across systems suggests evolutionary conservation in electron donor selection for DNRA optimization, likely driven by thermodynamic advantages and compatibility with the respiratory chain architecture. Future investigations employing quantitative proteomics and enzyme kinetic analyses will be conducted to elucidate the molecular mechanisms underlying the citrate-enhanced DNRA process.

3.2. Influence of C/N Ratio on the DNRA Performance of Strain LZ-1. Using sodium citrate as the carbon source, the effects of varying C/N ratios on the growth of strain LZ-1 and the DNRA process were assessed, as presented in Figure 2. As shown in Figure 2A, during the cultivation period, strain LZ-1 exhibited rapid growth at C/N ratios of 8 and 10, reaching the stationary phase at 32 and 40 h, respectively, with maximum OD_{600} values exceeding 1.6. In contrast, both low (C/N = 3 and 5) and high (C/N = 15 and 20) C/N ratios resulted in reduced growth rates and peak cell concentrations. Significant removal of NO_3^--N was achieved within 24 h across all C/N ratios, with complete removal occurring by 72 h (Figure 2B). As shown in Figure 2C, corresponding to the NO_3^--N removal, NO_2^--N rapidly accumulated and peaked within 24 h

https://doi.org/10.1021/acsomega.5c00470
ACS Omega 2025, 10, 16695−16704

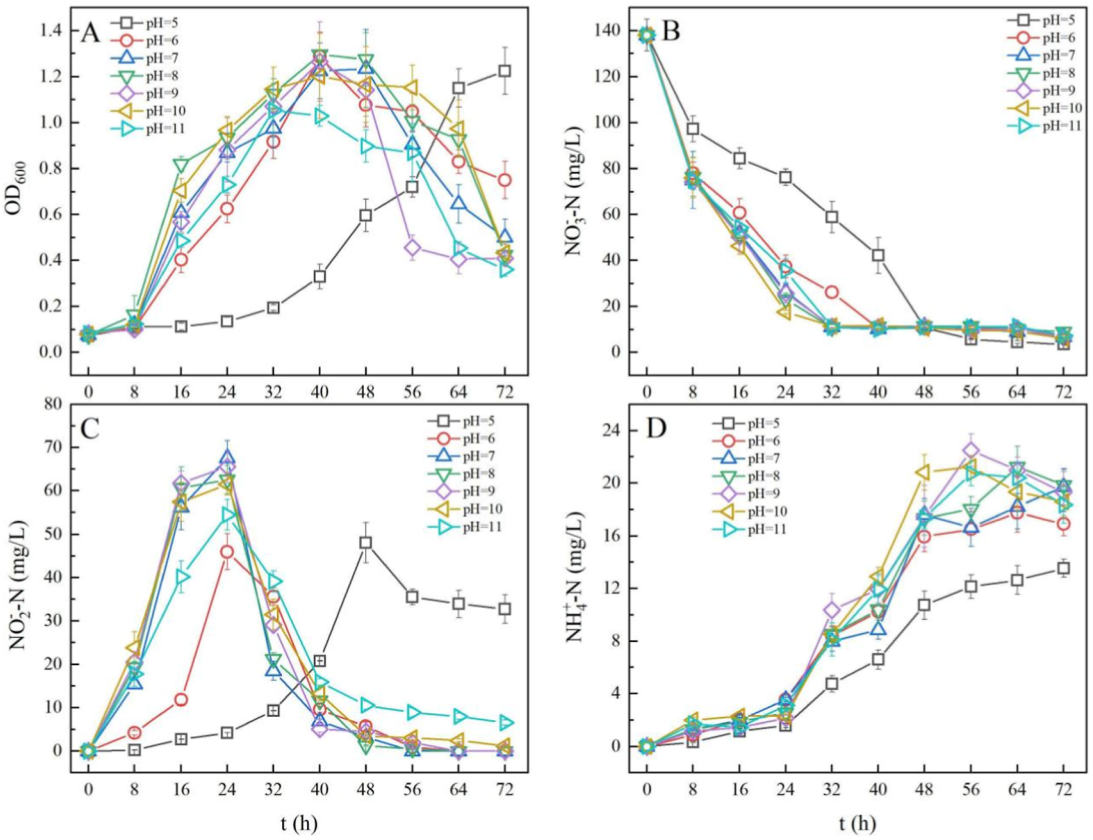

Figure 3. The growth and DNRA process of the strain LZ-1 under different initial pH. (A) OD_{600} changes, (B) NO_3^--N concentrations, (C) NO_2^--N concentrations, and (D) ammonium production.

at different C/N ratios. Subsequently, under C/N ratios of 8 and 10, the concentration of NO_2^--N in the culture rapidly decreased to 0 mg/L. The decrease of NO_2^--N was relatively slow at C/N ratios of 5, 15, and 20 but ultimately also reached 0 mg/L. However, at a C/N ratio of 3, a noticeable accumulation of NO_2^--N occurred, reaching a concentration of 38.19 mg/L at 72 h. Figure 2D illustrates that the ammonia nitrogen yields over 72 h ranked from highest to lowest as follows: C/N = 8 > C/N = 10 > C/N = 5 > C/N = 15 > C/N = 20 > C/N = 3. The ammonia nitrogen yield was the highest at a C/N ratio of 8, reaching 21.68 mg/L with an ammonia nitrogen yield efficiency of 15.71%. These findings indicate that strain LZ-1 exhibited optimal DNRA performance at a C/N ratio of 8.

The optimal DNRA performance of strain LZ-1 at C/N = 8 (15.71% NH_4^+-N yield) reflects balanced electron allocation between nitrite ammonification and biomass synthesis. In most studies, higher C/N ratios favor the DNRA process, regardless of whether a mixed microbial community or pure strains are used.[49−51] Low C/N = 3 induced NO_2^--N accumulation (Figure 2C), mirroring carbon-limited DNRA patterns in *Pseudomonas putida* Y-9[52] and *Shewanella loihica* PV-4,[28] where insufficient electron donors restrict eight-electron transfer to NH_4^+. Complete NO_2^--N depletion at C/N ≥ 5 demonstrates LZ-1's robust nitrite reductase activity across moderate-to-high C/N conditions. However, when the C/N ratio exceeded 8, the NH_4^+-N yields declined (Figure 2D), which aligns with the observations of *Pseudomonas stutzeri* strain XL-2 at elevated C/N ratios.[53] This may be correlated with metabolic flux shifts toward carbon storage and suppressed NrfA expression. In addition, the strain LZ-1's higher optimal C/N compared to *P. stutzeri* strain XL-2 (C/N = 5)[53] suggests species-specific variations in carbon utilization efficiency, potentially linked to TCA cycle regulation or nitrate reductase affinity.

3.3. Influence of Initial pH on the DNRA Performance of Strain LZ-1. When sodium citrate was employed as the carbon source, a C/N ratio of 8, and a temperature of 30 °C, the DNRA performance of strain LZ-1 was evaluated at different initial pH levels, with the results presented in Figure 3. As shown in Figure 3A, at an initial pH of 5, the growth of strain LZ-1 was very slow during the first 24 h, followed by entry into the logarithmic phase at 72 h and the stationary phase thereafter. When the initial pH ranged from 6 to 11, strain LZ-1 entered the logarithmic phase at 8 h and reached the stationary phase between 32 and 40 h. Notably, at an initial pH of 11, the maximum OD_{600} value of strain LZ-1 was approximately 1.0, which was lower than that observed at initial pH levels between 6 and 10. These results indicate that strain LZ-1 exhibited better growth within the pH range of 6 to 10. Figure 3B shows that at an initial pH of 5, the nitrate removal by the strain LZ-1 was slower, with a removal efficiency exceeding 92.2% after 48 h. At initial pH levels between 6 and 11, strain LZ-1 achieved over 91.60% nitrate removal within 32 to 40 h, which aligned with the bacterial growth patterns. In terms of nitrite accumulation, as seen in Figure 3C, at initial pH levels between 6 and 11, nitrite was rapidly accumulated within 24 h, and then it was rapidly transformed into the nitrite. At 64 h, with the exception of minor nitrite accumulation at initial pH levels of 10 and 11, strain LZ-1 completely transformed the accumulated nitrite at pH levels between 6 and 9. Regarding ammonium transformation, as depicted in Figure 3D, when the initial pH was

https://doi.org/10.1021/acsomega.5c00470
ACS Omega 2025, 10, 16695−16704

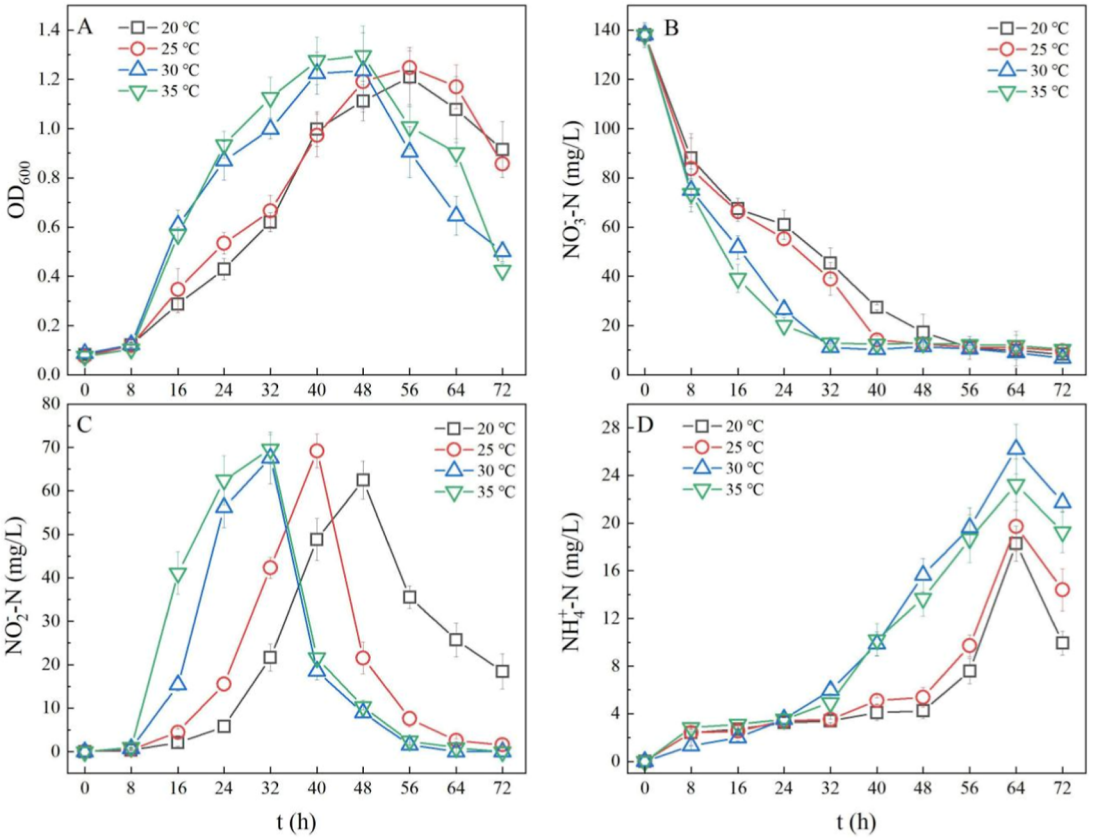

Figure 4. The cell growth and DNRA process of strain LZ-1 under different temperatures. (A) OD_{600} changes, (B) NO_3^--N concentrations, (C) NO_2^--N concentrations, and (D) ammonium production.

between 6 and 8, the ammonium production reached its maximum at 64 h, with yields of 12.87%, 14.28%, and 15.38%, respectively. At initial pH levels between 9 and 11, the maximum ammonium production occurred at 56 h, with yields of 16.30%, 15.39%, and 15.02%, respectively.

The enhanced DNRA performance of strain LZ-1 under alkaline conditions (pH 9−11) aligns with previous findings that elevated pH favors respiratory ammonification over denitrification.[28] The rapid nitrate removal and ammonium accumulation at pH 9−11 (Figure 3B,D) may be attributed to optimal enzymatic activity of NrfA, which typically exhibits higher efficiency in neutral to alkaline environments.[28,52] Notably, the peak ammonium yield at pH 9 (16.30%) mirrors observations in *P. putida* Y-9, where maximal nirBD expression and DNRA activity occurred at pH 7−9,[52] suggesting conserved pH-dependent regulatory mechanisms for DNRA enzymes across taxa. The transient nitrite accumulation at pH 10−11 (Figure 3C) likely reflects partial inhibition of NrfA-mediated nitrite reduction under extreme alkalinity, a phenomenon also reported in *S. loihica* PV-4 at pH > 8.0.[28] The exceptional capacity of strain LZ-1 to maintain DNRA activity across an extended pH spectrum (6.0−11.0) demonstrates considerable potential for enhancing nitrogen retention in wastewater treatment systems experiencing pH fluctuations. Future investigations employing proteomic analyses of pH-responsive pathways, coupled with structural−functional studies of its enzymatic machinery, are required to elucidate the molecular adaptations underlying this pH resilience and optimize its application.

3.4. Effect of Temperature on the DNRA Performance of the Strain LZ-1. Under experimental conditions utilizing sodium citrate as the carbon source, a C/N ratio of 8, and an initial pH of 9, the influence of varying temperatures (20 °C, 25 °C, 30 °C, and 35 °C) on the DNRA performance of strain LZ-1 was investigated, as illustrated in Figure 4. Figure 4A demonstrates that the growth rate of strain LZ-1 at 30 and 35 °C was significantly higher than that at 20 and 25 °C, with a marginally greater maximum bacterial density (OD_{600}) observed in the stationary phase. Moreover, the growth rate and bacterial density during the stationary phase at 35 °C were slightly superior to those at 30 °C. In terms of nitrate removal (Figure 4B), after 72 h of incubation at all tested temperatures, strain LZ-1 achieved nitrate removal efficiencies exceeding 92.51%. Notably, at 30 and 35 °C, the strain removed 92.03% and 90.72% of nitrate within 32 h, respectively, indicating faster removal rates compared to 20 and 25 °C. Regarding nitrite accumulation (Figure 4C), strain LZ-1 peaked in nitrite accumulation at 32 h at 30 and 35 °C, followed by complete removal by 64 and 72 h, respectively, with no accumulation detected. In contrast, at 20 and 25 °C, peak nitrite accumulation occurred at 48 and 40 h, respectively, with residual nitrite remaining after 72 h. Concerning ammonium transformation (Figure 4D), the rate and yield of ammonium production were the highest at 30 °C, reaching a maximum of 26.21 mg/L at 64 h, with an ammonia yield efficiency of 18.99%. As previously reported, elevated temperatures promote the DNRA process.[45,54] Similarly, this study found that higher temperatures (30 and 35 °C) enhanced the DNRA performance of the strain LZ-1 compared to 20 and 25 °C. However, a raise in temperature from 30 to 35 °C resulted in a decrease in ammonium production, potentially due to strain LZ-1's nitrite reductase showing a preference for 30 °C. These

https://doi.org/10.1021/acsomega.5c00470
ACS Omega 2025, 10, 16695−16704

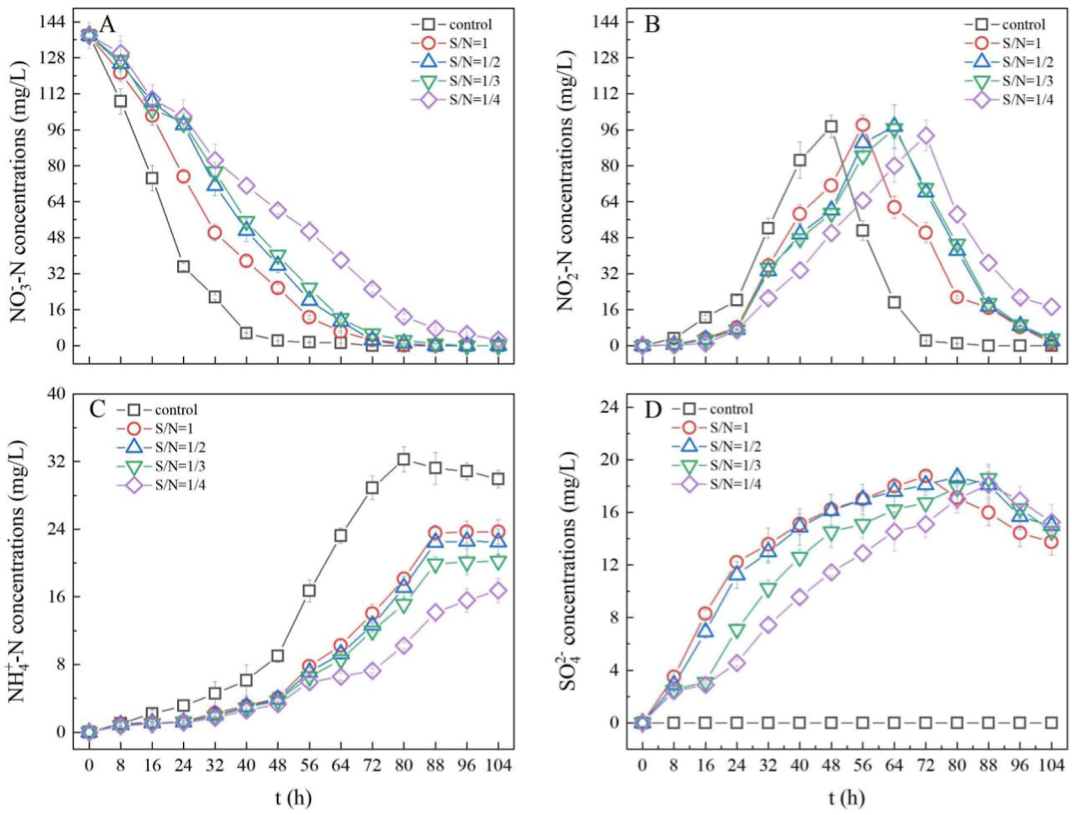

Figure 5. The influence of S^{2-} on the DNRA process of strain LZ-1. (A) NO_3^--N concentrations, (B) NO_2^--N concentrations, (C) ammonium production, and (D) SO_4^{2-} concentrations.

results indicate that under the conditions of sodium citrate as the carbon source, a C/N ratio of 8, an initial pH of 9, and a temperature of 30 °C, the strain LZ-1 exhibits optimal DNRA performance.

3.5. Effect of S^{2-}/N on the DNRA Performance of the Strain LZ-1. The influence of varying S/N (S^{2-}) ratios on the DNRA performance of the strain LZ-1 was investigated under conditions using sodium citrate as the carbon source, a C/N ratio of 8, an initial pH of 9, and a temperature of 30 °C. The results are presented in Figure 5. As shown in Figure 5A, compared to the control group, the addition of S^{2-} prolonged the time required for complete nitrate removal by strain LZ-1, indicating a negative effect of S^{2-} on nitrate reduction. However, this inhibitory effect appeared to increase as the S/N ratio decreased. Similarly, the addition of S^{2-} also had a detrimental effect on nitrite reduction (Figure 5B). In the presence of S^{2-}, the appearances of peak nitrite concentration were delayed by more than 8 h compared to the control group, and incomplete nitrite removal was observed. At different S/N ratios, the time to reach the peak nitrite concentration followed the following trend: S/N = 1 < S/N = 1/2 = S/N = 1/3 < S/N = 1/4, which is consistent with the NO_3^--N removal shown in Figure 5A. At the end of the culture (104 h), the accumulated nitrite concentrations at S/N ratios of 1, 1/2, 1/3, and 1/4 were 1.26 mg/L, 2.12 mg/L, 3.11 mg/L, and 17.23 mg/L, respectively. These results suggest that a low S/N ratio (S/N = 1/4) significantly impaired both the production and removal of nitrite, with the negative impact diminishing as the S/N ratio increased. As can be seen in Figure 5C, compared to the control group, the presence of S^{2-} markedly reduced ammonia production by strain LZ-1. The maximum ammonia yield efficiency in the control group was 23.36%, while at S/N ratios of 1, 1/2, 1/3, and 1/4, the maximum ammonia yield efficiencies were 17.17%, 16.35%, 14.66%, and 12.15%, respectively. This indicates that as the S/N ratio decreased, ammonia production gradually declined, consistent with the nitrite accumulation observed at different S/N ratios. Specifically, at low S/N ratios, more nitrite accumulated, resulting in less ammonia production from nitrite reduction. Figure 5D shows that SO_4^{2-} was detected in all of the S^{2-}-added experimental groups. Since no sulfate is present in the modified SM medium, the SO_4^{2-} likely originates from the conversion of S^{2-}, which is consistent with the trend of decreasing S^{2-} concentration (see Figure S4). This suggests that the strain LZ-1 may utilize S^{2-} as an electron donor to reduce NO_3^- to NH_4^+ while producing SO_4^{2-}.[55,56] The SO_4^{2-} production rate increased with the S/N ratio, indicating that at higher S/N ratios, the strain's metabolic regulation accelerated the conversion of S^{2-} to SO_4^{2-}.

These findings suggest that the addition of S^{2-} inhibited the DNRA process in strain LZ-1, including reducing the rate of nitrate to nitrite conversion and inhibiting nitrite reduction to ammonia, ultimately leading to decreased ammonia production. These observations are consistent with previous studies reporting that sulfur ions inhibit DNRA.[44,57] It is reported that sulfide binds to metal centers of heme-containing enzymes, such as Nar and Nap, inactivating these enzymes and disrupting nitrogen conversion.[58] Additionally, sulfide inhibits Nar and Nir by competing with nitrate/nitrite as an electron donor or directly poisoning metalloenzymes, thereby reducing NO_3^-/NO_2^- reduction efficiency.[59] Furthermore, sulfide-induced oxidative stress damages cellular components like DNA and proteins, exacerbating metabolic dysfunction.[60] While the previously reported inhibitory mechanisms of

https://doi.org/10.1021/acsomega.5c00470
ACS Omega 2025, 10, 16695−16704

sulfides on bacterial nitrogen conversion may partially explain the significant decline in DNRA performance observed with sulfide addition compared to the control group without sulfide addition, these established models show two critical limitations: (1) they cannot explain the dose-dependent attenuation of sulfide toxicity observed at elevated S/N ratios (Figure 5C), and (2) they fail to reconcile the concomitant S^{2-} decline and SO_4^{2-} accumulation patterns (Figures S4 and 5D). This apparent S/N ratio-dependent detoxification phenomenon suggests that strain LZ-1 activates adaptive metabolic pathways. Building on sulfur-handling strategies in *Gordonia* sp. TD-4[17] and *Desulfurivibrio alkaliphilus*[61]—which coordinately execute DNRA and sulfide oxidation—it is hypothesized that strain LZ-1 employs S^{2-} as dual-purpose substrates: (1) electron donors for DNRA-mediated nitrate reduction[58] and (2) sulfur sources oxidized to SO_4^{2-} through pathways potentially involving SQR or other sulfur-oxidizing enzymes. This metabolic flexibility would simultaneously alleviate sulfide inhibition and sustain nitrogen transformation. Future investigations focus on enzyme kinetics (e.g., SQR activities under varying S/N conditions), and transcriptomic profiling to identify sulfur metabolism gene clusters will be carried out to validate these sulfur-handling pathways.

4. CONCLUSIONS

The study investigates the impact of environmental factors on the DNRA bacterium using strain LZ-1 as a model. The findings indicate that the optimal performance of DNRA by this strain is achieved under conditions where sodium citrate serves as the organic carbon source, with a C/N ratio of 8, an initial pH of 9, and a temperature of 30 °C. The presence of sulfur ions inhibits the DNRA process in strain LZ-1. However, this inhibitory effect diminishes as the S/N ratio increases. These results contribute to a deeper insight into how environmental factors influence the DNRA process, providing theoretical support for the subsequent recovery of nitrogen from nitrate-containing wastewater through DNRA.

■ ASSOCIATED CONTENT

Supporting Information

The Supporting Information is available free of charge at https://pubs.acs.org/doi/10.1021/acsomega.5c00470.

Details of screening, domestication, and identification of functional strains and variation of S^{2-} concentration (PDF)

■ AUTHOR INFORMATION

Corresponding Author

Zhen-Jun Wu − *School of Environmental Engineering, Henan University of Technology, Zhengzhou 450001, China;* orcid.org/0000-0002-0341-8977; Phone: +86-13629841966; Email: wuzhenjun@haut.edu.cn

Authors

Teng-Fei Ma − *National Research Base of Intelligent Manufacturing Service, Chongqing Technology and Business University, Chongqing 400067, China;* orcid.org/0000-0001-5592-9544

Xiao-Yao Yu − *National Research Base of Intelligent Manufacturing Service, Chongqing Technology and Business University, Chongqing 400067, China*

Chong-Yang Xing − *School of Environment and Resource, Chongqing Technology and Business University, Chongqing 400067, China*

Zhen Liu − *School of Environmental Engineering, Henan University of Technology, Zhengzhou 450001, China*

You-Peng Chen − *Key Laboratory of the Three Gorges Reservoir Region's Eco-Environment, Ministry of Education, Chongqing University, Chongqing 400045, China;* orcid.org/0000-0002-7332-7464

Complete contact information is available at: https://pubs.acs.org/10.1021/acsomega.5c00470

Notes

The authors declare no competing financial interest.

■ ACKNOWLEDGMENTS

This study was financed by the National Natural Science Foundation of China (42207243), the Key Research and Development Project of Henan Province (242102320087), the Chongqing Natural Science Foundation project (CSTB2023NSCQ-MSX0963), and the Chongqing Technology and Business University Research Program (2056021). We extend our gratitude to ChatGLM (developed by Zhipu Qingyan, Beijing Knowledge Atlas Technology Co., Ltd.) for its assistance in enhancing the quality of our writing during the preparation of this manuscript.

■ REFERENCES

(1) Mateo, D.; Sousa, A.; Zakharzhevskii, M.; Gascon, J. Challenges and opportunities for the photo-(thermal) synthesis of ammonia. *Green Chem.* **2024**, *26*, 1041−1061.

(2) Wang, Y.; Meyer, T. J. A Route to Renewable Energy Triggered by the Haber-Bosch Process. *Chem* **2019**, *5*, 496.

(3) Hermann, A. Haber und Bosch: Brot aus Luft - Die Ammoniaksynthese. *Physik. Blätter* **1965**, *21*, 168−171.

(4) Suryanto, B. H. R.; Du, H.-L.; Wang, D.; Chen, J.; Simonov, A. N.; MacFarlane, D. R. Challenges and prospects in the catalysis of electroreduction of nitrogen to ammonia. *Nat. Catal.* **2019**, *2*, 290.

(5) Xu, S.; Wu, X.; Lu, H. Overlooked nitrogen-cycling microorganisms in biological wastewater treatment. *Front. Environ. Sci. Eng.* **2021**, *15*, 133.

(6) Zhao, L.; Chen, J.; Shen, G.; Zhou, Y.; Zhang, X.; Zhou, Y.; Yu, Z.; Ma, J. Dissimilatory nitrate reduction to ammonia in the natural environment and wastewater treatment facilities: A comprehensive review. *Environ. Technol. Innovation* **2025**, *37*, 104011.

(7) Chen, Y.; Wang, F. Insights on nitrate respiration by Shewanella. *Front. Mar. Sci.* **2015**, *1 -2014*, DOI: 10.3389/fmars.2014.00080.

(8) Chovanec, P.; Sparacino-Watkins, C.; Zhang, N.; Basu, P.; Stolz, J. F. Microbial Reduction of Chromate in the Presence of Nitrate by Three Nitrate Respiring Organisms. *Front. Microbiol.* **2012**, *3*, 416.

(9) Hanson, T. E.; Campbell, B. J.; Kalis, K. M.; Campbell, M. A.; Klotz, M. G. Nitrate ammonification by Nautilia profundicola AmH: experimental evidence consistent with a free hydroxylamine intermediate. *Front. Microbiol.* **2013**, *4*, 180.

(10) Simon, J. Enzymology and bioenergetics of respiratory nitrite ammonification. *FEMS Microbiol. Rev.* **2002**, *26*, 285−309.

(11) Campbell, B. J.; Smith, J. L.; Hanson, T. E.; Klotz, M. G.; Stein, L. Y.; Lee, C. K.; Wu, D.; Robinson, J. M.; Khouri, H. M.; Eisen, J. A.; et al. Adaptations to Submarine Hydrothermal Environments Exemplified by the Genome of Nautilia profundicola. *PLoS Genet.* **2009**, *5*, No. e1000362.

(12) Wen, W.-R.; Liu, T.-C.; Fan, S.-Q.; Tan, X.; Lu, Y.; Xing, D.-F.; Liu, B.-F.; Ren, N.-Q.; Xie, G.-J. Dissimilatory nitrate reduction to ammonium driven by different electron donors: Mechanisms, recent advances, and future perspectives. *Chem. Eng. J.* **2025**, *507*, 160625.

(13) Zhang, Y.; Wang, B.; Puig, S.; Tong, Y.; Zhao, Y.; Zhai, S. Capturing wastewater nitrogen through METs-assisted dissimilatory nitrate reduction to ammonium (DNRA) using various electron donors: Recent Trends, challenges, and future directions. *Chem. Eng. J.* **2024**, *501*, 157597.
(14) Pandey, C. B.; Kumar, U.; Kaviraj, M.; Minick, K. J.; Mishra, A. K.; Singh, J. S. DNRA: A short-circuit in biological N-cycling to conserve nitrogen in terrestrial ecosystems. *Sci. Total Environ.* **2020**, *738*, 139710.
(15) Lu, W.-W.; Zhang, H.-L.; Shi, W.-M. Dissimilatory nitrate reduction to ammonium in an anaerobic agricultural soil as affected by glucose and free sulfide. *Eur. J. Soil Biol.* **2013**, *58*, 98−104.
(16) Fernandes, S. O.; Bonin, P. C.; Michotey, V. D.; Garcia, N.; LokaBharathi, P. A. Nitrogen-limited mangrove ecosystems conserve N through dissimilatory nitrate reduction to ammonium. *Sci. Rep.* **2012**, *2*, 419.
(17) Qi, P.; Sun, D.; Zhang, G.; Li, D.; Wu, T.; Li, Y. Bio-augmentation with dissimilatory nitrate reduction to ammonium (DNRA) driven sulfide-oxidizing bacteria enhances the durability of nitrate-mediated souring control. *Water Res.* **2022**, *219*, 118556.
(18) Xie, Y.; Wang, Z.; Ismail, S.; Ni, S.-Q. Long-term operation and dynamic response of dissimilatory nitrate reduction to ammonium process under low-frequency infrared electromagnetic field. *npj Clean Water* **2024**, *7*, 60.
(19) Zhou, L.; Zhao, B.; Zhuang, W.-Q. Double-edged sword effects of dissimilatory nitrate reduction to ammonium (DNRA) bacteria on anammox bacteria performance in an MBR reactor. *Water Res.* **2023**, *233*, 119754.
(20) Wang, C.; Qiao, S.; Bi, Z.; Zhou, J. Nitrate removal by anammox biomass with intracellular carbon source as electron donors via DNRA pathway. *Environ. Res.* **2021**, *200*, 111390.
(21) Eltaweil, A. S.; Omer, A. M.; El-Aqapa, H. G.; Gaber, N. M.; Attia, N. F.; El-Subruiti, G. M.; Mohy-Eldin, M. S.; Abd El-Monaem, E. M. Chitosan based adsorbents for the removal of phosphate and nitrate: A critical review. *Carbohydr. Polym.* **2021**, *274*, 118671.
(22) Li, X.; Gu, Y.; Wu, S.; Chen, S.; Quan, X.; Yu, H. Selective reduction of nitrate to ammonium over charcoal electrode derived from natural wood. *Chemosphere* **2021**, *285*, 131501.
(23) Thamdrup, B. New Pathways and Processes in the Global Nitrogen Cycle. *Annu. Rev. Ecol. Evol. Syst.* **2012**, *43*, 407.
(24) Lin, J. T.; Stewart, V. Nitrate Assimilation by Bacteria. In *Advances in Microbial Physiology*; Poole, R. K., Ed.; Academic Press, 1997; pp 1−30.
(25) Zhao, Y.; Li, Q.; Cui, Q.; Ni, S.-Q. Nitrogen recovery through fermentative dissimilatory nitrate reduction to ammonium (DNRA): Carbon source comparison and metabolic pathway. *Chem. Eng. J.* **2022**, *441*, 135938.
(26) Wan, Y.; Huang, Z.; Zhou, L.; Li, T.; Liao, C.; Yan, X.; Li, N.; Wang, X. Bioelectrochemical Ammoniation Coupled with Microbial Electrolysis for Nitrogen Recovery from Nitrate in Wastewater. *Environ. Sci. Technol.* **2020**, *54*, 3002−3011.
(27) Wang, Z.; Bu, C.; Dou, J.; Ismail, S.; Ahmad, S.; Qi, D.; Wei, H.; Chen, X.; Lee, T.; Tawfik, A.; et al. Enrichment of DNRA bacteria: Shift of microbial community and its combination with anammox to promote TN removal. *J. Environ. Chem. Eng.* **2022**, *10*, 108867.
(28) Yoon, S.; Cruz-García, C.; Sanford, R.; Ritalahti, K. M.; Löffler, F. E. Denitrification versus respiratory ammonification: environmental controls of two competing dissimilatory NO_3^-/NO_2^- reduction pathways in *Shewanella loihica* strain PV-4. *ISME J.* **2015**, *9*, 1093−1104.
(29) Carlson, H. K.; Lui, L. M.; Price, M. N.; Kazakov, A. E.; Carr, A. V.; Kuehl, J. V.; Owens, T. K.; Nielsen, T.; Arkin, A. P.; Deutschbauer, A. M. Selective carbon sources influence the end products of microbial nitrate respiration. *ISME J.* **2020**, *14*, 2034−2045.
(30) Huang, X.; Tie, W.; Xie, D.; Li, Z. Low C/N Ratios Promote Dissimilatory Nitrite Reduction to Ammonium in Pseudomonas putida Y-9 under Aerobic Conditions. *Microorganisms* **2021**, *9*, 1524.
(31) Li, S.; Jiang, Z.; Ji, G. Effect of sulfur sources on the competition between denitrification and DNRA. *Environ. Pollut.* **2022**, *305*, 119322.
(32) Rahman, M.; Grace, M. R.; Roberts, K. L.; Kessler, A. J.; Cook, P. L. M. Effect of temperature and drying-rewetting of sediments on the partitioning between denitrification and DNRA in constructed urban stormwater wetlands. *Ecol. Eng.* **2019**, *140*, 105586.
(33) Stevens, R. J.; Laughlin, R. J.; Malone, J. P. Soil pH affects the processes reducing nitrate to nitrous oxide and di-nitrogen. *Soil Biol. Biochem.* **1998**, *30*, 1119−1126.
(34) Schmidt, C. S.; Richardson, D. J.; Baggs, E. M. Constraining the conditions conducive to dissimilatory nitrate reduction to ammonium in temperate arable soils. *Soil Biol. Biochem.* **2011**, *43*, 1607−1611.
(35) Kraft, B.; Tegetmeyer, H. E.; Sharma, R.; Klotz, M. G.; Ferdelman, T. G.; Hettich, R. L.; Geelhoed, J. S.; Strous, M. The environmental controls that govern the end product of bacterial nitrate respiration. *Science* **2014**, *345*, 676−679.
(36) van den Berg, E. M.; Elisário, M. P.; Kuenen, J. G.; Kleerebezem, R.; van Loosdrecht, M. C. M. Fermentative Bacteria Influence the Competition between Denitrifiers and DNRA Bacteria. *Front. Microbiol.* **2017**, *8*, 1684.
(37) Chutivisut, P.; Isobe, K.; Powtongsook, S.; Pungrasmi, W.; Kurisu, F. Distinct Microbial Community Performing Dissimilatory Nitrate Reduction to Ammonium (DNRA) in a High C/NO_3^- Reactor. *Microbes Environ.* **2018**, *33*, 264−271.
(38) Dolejs, P.; Paclík, L.; Maca, J.; Pokorna, D.; Zabranska, J.; Bartacek, J. Effect of S/N ratio on sulfide removal by autotrophic denitrification. *Appl. Microbiol. Biotechnol.* **2015**, *99*, 2383−2392.
(39) Brunet, R. C.; Garcia-Gil, L. J. Sulfide-induced dissimilatory nitrate reduction to ammonia in anaerobic freshwater sediments. *FEMS Microbiol. Ecol.* **1996**, *21*, 131−138.
(40) Yin, Z.; Xie, L.; Zhou, Q. Effects of sulfide on the integration of denitrification with anaerobic digestion. *J. Biosci. Bioeng.* **2015**, *120*, 426−431.
(41) Senga, Y.; Mochida, K.; Fukumori, R.; Okamoto, N.; Seike, Y. N_2O accumulation in estuarine and coastal sediments: The influence of H2S on dissimilatory nitrate reduction. *Estuarine, Coastal Shelf Sci.* **2006**, *67*, 231−238.
(42) Murphy, A. E.; Bulseco, A. N.; Ackerman, R.; Vineis, J. H.; Bowen, J. L. Sulphide addition favours respiratory ammonification (DNRA) over complete denitrification and alters the active microbial community in salt marsh sediments. *Environ. Microbiol.* **2020**, *22*, 2124−2139.
(43) Tuerk, K. J. S.; Aelion, C. M. Microbial nitrogen removal in a developing suburban estuary along the South Carolina coast. *Estuaries* **2005**, *28*, 364−372.
(44) Dalsgaard, T.; Bak, F. Nitrate Reduction in a Sulfate-Reducing Bacterium, Desulfovibrio desulfuricans, Isolated from Rice Paddy Soil: Sulfide Inhibition, Kinetics, and Regulation. *Appl. Environ. Microbiol.* **1994**, *60*, 291−297.
(45) Lai, T. V.; Ryder, M. H.; Rathjen, J. R.; Bolan, N. S.; Croxford, A. E.; Denton, M. D. Dissimilatory nitrate reduction to ammonium increased with rising temperature. *Biol. Fertil. Soils* **2021**, *57*, 363−372.
(46) Nepa, C. *Water and Wastewater Monitoring and Analysis Methods*, 4th ed.; Chinese Environmental Science Publishing House: Beijing, 2002.
(47) Tugtas, A. E.; Pavlostathis, S. G. Electron donor effect on nitrate reduction pathway and kinetics in a mixed methanogenic culture. *Biotechnol. Bioeng.* **2007**, *98*, 756−763.
(48) Strohm, T. O.; Griffin, B.; Zumft, W. G.; Schink, B. Growth Yields in Bacterial Denitrification and Nitrate Ammonification. *Appl. Environ. Microbiol.* **2007**, *73*, 1420−1424.
(49) Algar, C.; Vallino, J. Predicting microbial nitrate reduction pathways in coastal sediments. *Aquat. Microb. Ecol.* **2014**, *71*, 223−238.
(50) Domangue, R. J.; Mortazavi, B. Nitrate reduction pathways in the presence of excess nitrogen in a shallow eutrophic estuary. *Environ. Pollut.* **2018**, *238*, 599−606.

https://doi.org/10.1021/acsomega.5c00470
ACS Omega 2025, 10, 16695−16704

(51) Liu, S.; Dai, J.; Wei, H.; Li, S.; Wang, P.; Zhu, T.; Zhou, J.; Qiu, D. Dissimilatory Nitrate Reduction to Ammonium (DNRA) and Denitrification Pathways Are Leveraged by Cyclic AMP Receptor Protein (CRP) Paralogues Based on Electron Donor/Acceptor Limitation in Shewanella loihica PV-4. *Appl. Environ. Microbiol.* **2021**, *87*, No. e01964.
(52) Huang, X.; Tie, W.; Xie, D.; Jiang, D.; Li, Z. Certain Environmental Conditions Maximize Ammonium Accumulation and Minimize Nitrogen Loss During Nitrate Reduction Process by Pseudomonas putida Y-9. *Front. Microbiol.* **2021**, *12*, 764241.
(53) Zhao, B.; Cheng, D. Y.; Tan, P.; An, Q.; Guo, J. S. Characterization of an aerobic denitrifier Pseudomonas stutzeri strain XL-2 to achieve efficient nitrate removal. *Bioresour. Technol.* **2018**, *250*, 564−573.
(54) Wei, Z.; Jin, K.; Li, C.; Wu, M.; Shan, J.; Yan, X. Environmental Factors Controlling Dissimilatory Nitrate Reduction to Ammonium in Paddy Soil. *J. Soil Sci. Plant Nutr.* **2022**, *22*, 4241−4248.
(55) Sayama, M.; Risgaard-Petersen, N.; Nielsen, L. P.; Fossing, H.; Christensen, P. B. Impact of Bacterial NO_3^- Transport on Sediment Biogeochemistry. *Appl. Environ. Microbiol.* **2005**, *71*, 7575−7577.
(56) Yuan, H.; Jia, B.; Zeng, Q.; Zhou, Y.; Wu, J.; Wang, H.; Fang, H.; Cai, Y.; Li, Q. Dissimilatory nitrate reduction to ammonium (DNRA) potentially facilitates the accumulation of phosphorus in lake water from sediment. *Chemosphere* **2022**, *303*, 134664.
(57) McCready, R. G. L.; Gould, W. D.; Cook, F. D. Respiratory nitrate reduction by Desulfovibrio sp. *Arch. Microbiol.* **1983**, *135*, 182−185.
(58) Wang, D.; Xu, S.; Jiang, C.; Wang, X.; Yang, D.; Kuai, B.; Zhuang, X. The effects, mechanisms, and applications of sulfide as both an inhibitor and electron donor in novel biological nitrogen removal process. *Sci. Total Environ.* **2023**, *894*, 164784.
(59) Feng, Y.; Zhang, X.; Zhang, C.; Xu, H.; Ji, X.; Wang, J.; Wu, P.; Qian, F.; Chen, C.; Shen, Y.; et al. Roles of waste iron scraps in anammox system treating sulfide-containing wastewater: Alleviating sulfide inhibition, promoting novel anammox bacteria enrichment, and enhancing nitrogen removal capacity. *Bioresour. Technol.* **2025**, *419*, 132033.
(60) Jin, R.-C.; Yang, G.-F.; Zhang, Q.-Q.; Ma, C.; Yu, J.-J.; Xing, B.-S. The effect of sulfide inhibition on the ANAMMOX process. *Water Res.* **2013**, *47*, 1459−1469.
(61) Thorup, C.; Schramm, A.; Findlay, A. J.; Finster, K. W.; Schreiber, L. Disguised as a Sulfate Reducer: Growth of the Deltaproteobacterium Desulfurivibrio alkaliphilus by Sulfide Oxidation with Nitrate. *mBio* **2017**, *8*, No. e00671.

https://doi.org/10.1021/acsomega.5c00470
ACS Omega 2025, 10, 16695−16704